Physics Letters B 808 (2020) 135627

Contents lists available at ScienceDirect

Physics Letters B

www.elsevier.com/locate/physletb

Physical resurgent extrapolation

Ovidiu Costin [a], Gerald V. Dunne [b]

[a] Department of Mathematics, The Ohio State University, Columbus, OH 43210-1174, USA
[b] Department of Physics, University of Connecticut, Storrs, CT 06269-3046, USA

ARTICLE INFO

Article history:
Received 1 June 2020
Received in revised form 13 July 2020
Accepted 13 July 2020
Available online 17 July 2020
Editor: A. Volovichis

ABSTRACT

Expansions of physical functions are controlled by their singularities, which have special structure because they themselves are physical, corresponding to instantons, caustics or saddle configurations. Resurgent asymptotics formalizes this idea mathematically, and leads to significantly more powerful extrapolation methods to extract physical information from a finite number of terms of an expansion, including precise decoding of non-perturbative effects. We quantify the gain of precision for various extrapolation procedures, showing that significant improvements can be achieved using exactly the same input data, and we illustrate the general method with examples from quantum mechanics and quantum field theory.

An important problem in physics is the following: given a physical quantity (free energy, correlator, scattering amplitude, ...) expanded in a parameter (temperature, distance, coupling, ...) to a *finite* number of terms in some parametric limit, we wish to extract as much physical information as possible about the function in other parametric regimes [1–19]. For e.g., an extrapolation between weak and strong coupling, real and complex fugacity, or Euclidean and Minkowski space. Note that for these latter two problems we need methods that can also extrapolate in the complex domain. The original expansion may be convergent, but in many practical cases it is the start of an asymptotic series. If computing further terms is not possible, such an extrapolation appears to be a prohibitively difficult task. However, the series expansions of *physical* functions are not completely generic; they have further structure which we can exploit. This extra structure arises because saddle points and critical points have physical meaning, and tend to align and interact in specific ways. Mathematically, this extra structure follows from recent work in resurgent asymptotics [20–22] which shows that functions arising as solutions to systems of equations (differential, difference, integral, ...), generally have special orderly structure in the Borel plane. Resurgence implies that global information can be decoded from the original expansion coefficients. Some ingredients of our analysis are familiar: Borel summation, Padé approximation, conformal mapping, asymptotics of orthogonal polynomials, capacity theory, but we combine these in new ways. This leads to new quantitative measures of the precision of different extrapolations, and novel strategies for decoding non-perturbative physics from limited perturbative information. This motivates the use of resurgence as a discovery tool, an approach with a steadily growing body of evidence in a wide variety of branches of physics [23–40].

A broad class of physical problems involves analyzing a *finite* number of terms of an expansion of a function in a physical variable x, computed in the limit $x \to +\infty$:

$$F_{2N}(x) = \sum_{n=0}^{2N} \frac{a_n}{x^{n+1}} \quad , \quad x \to +\infty \tag{1}$$

Often this is an asymptotic expansion, with factorial leading large order behavior [41–44]:

$$a_n \sim (-1)^n \frac{\Gamma(n-\alpha)}{S^n} \quad , \quad n \to \infty \tag{2}$$

We illustrate our results with this divergent structure because of its physical relevance, but the general results extend to all resurgent functions [45]. This is ultimately because resurgent functions have isolated algebraic or logarithmic Borel branch points, each associated with asymptotic behavior of the form (2). The parameters S and α in (2) have physical meaning: S is related to the action of a dominant saddle configuration, and α to the power of x in the prefactor from fluctuations about this configuration. We have deliberately chosen the coefficients a_n to be alternating in sign, in order to begin our analysis as far as possible from a Stokes line, since one of our goals is to probe a non-perturbative Stokes transition by extrapolating from a *distant* perturbative regime.

E-mail address: gerald.dunne@uconn.edu (G.V. Dunne).

https://doi.org/10.1016/j.physletb.2020.135627

Table 1
The scaling with truncation order parameter N of the minimum real x value at which a chosen precision can be obtained, for each of the five extrapolation methods discussed here.

Extrapolation	$x_{\min}$ scaling
truncated series	$x_{\min} \sim N$
x Padé	$x_{\min} \sim N^{-1}$
Padé-Borel	$x_{\min} \sim N^{-2}$
Taylor-Conformal-Borel	$x_{\min} \sim N^{-2}$
Padé-Conformal-Borel	$x_{\min} \sim N^{-4}$

There are (at least[1]) 5 natural methods for extrapolating the truncated asymptotic expansion (1): (i) $F_{2N}(x)$ itself; (ii) Padé in the physical x plane; (iii) Borel-Padé: Padé in the Borel p plane; (iv) Taylor-Conformal-Borel: truncated series in the conformally mapped Borel plane; (v) Padé-Conformal-Borel: Padé of truncated series in conformally mapped Borel plane. We show that these are listed in order of increasing precision. We stress that each method begins with exactly the same input data: the truncated series (1). The only difference is the different *decoding* of the information contained in the input coefficients a_n. We quantify the quality of each extrapolation method with a concrete example that captures the Bender-Wu-Lipatov asymptotics in (2) (we scale x to set $S = 1$)

$$F(x;\alpha) = \frac{e^x \Gamma(1+\alpha, x)}{x^{1+\alpha}} \sim \sum_{n=0}^{\infty} \frac{(-1)^n \Gamma(n-\alpha)}{\Gamma(-\alpha) x^{n+1}} \tag{3}$$

$\Gamma(\beta, x)$ is the incomplete gamma function. $F(x;\alpha)$ has a branch cut (with parameter α) along the negative x axis, far from our perturbative $x \to +\infty$ expansion region, with a non-perturbative Stokes jump across the cut:

$$F(e^{i\pi} x;\alpha) - F(e^{-i\pi} x;\alpha) = \frac{-2\pi i}{\Gamma(-\alpha)} \frac{e^{-x}}{x^{1+\alpha}} \tag{4}$$

We probe: (i) extrapolation from $x = +\infty$ down to $x = 0$; (ii) extrapolation into the complex plane, rotating from the positive to negative real x axis. Case (i) is an analog of a high to low temperature extrapolation, and (ii) is an analog of a non-perturbative Stokes transition, like (4).

As mentioned above, the methods discussed here generalize to any resurgent function, as we can apply these tools *locally* by "zooming in" to the vicinity of any chosen Borel singularity. This, together with the fact that we are able to *quantify* the improvement in precision as the number of input coefficients changes, explains why we describe the extrapolation methods for the representative function in (3). We show below several examples to illustrate that the methods described here apply also to general cases with more than one contribution to the large-order behavior, due to multiple (indeed, infinitely many) Borel branch cuts.

The crudest approach is to use the truncated series (1), but the principle of least-term truncation [48] implies one can typically only extrapolate from $x \to +\infty$ down to $x_{\min} \sim N$. Padé approximation in x yields a significant improvement. Padé is a simple algorithmic re-processing of the input coefficients a_n [48,49]. For $F(x;\alpha)$ in (3), Padé can be written in closed-form in terms of Laguerre polynomials, using the fundamental connection between Padé and orthogonal polynomials (App. A). Large N asymptotics of Laguerre polynomials leads to a uniform estimate for the fractional error, implying that a desired level of precision can be achieved down to a minimum x that scales with the truncation order as $x_{\min} \sim 1/N$. See Fig. 1.

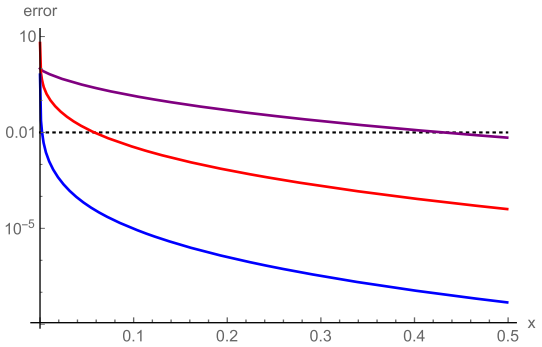

Fig. 1. Log plot of the fractional error in $F(x;-\frac{1}{3})$, extrapolated to $x \to 0^+$, with just 10 input coefficients ($N = 5$) from $x \to +\infty$. The horizontal line represents 1% fractional error. The purple, red and blue curves are the x plane Padé, Padé-Borel and Padé-Conformal-Borel extrapolations, respectively. Processing the same input data in different ways can yield vastly different extrapolation quality.

Borel methods directly yield a further $\frac{1}{N}$ factor improvement. See Fig. 1. We stress that this improvement of precision is based on exactly the same input data: it is just that the input truncated expansion is processed differently. The truncated Borel transform, $B_{2N}(p) \equiv \sum_{n=0}^{2N} \frac{a_n}{n!} p^n$, regenerates the original truncated series by a Laplace transform: $F_{2N}(x) = \int_0^\infty dp\, e^{-px} B_{2N}(p)$. Borel *extrapolation* is achieved by analytic continuation of the truncated Borel transform $B_{2N}(p)$. The quality of this continuation in the Borel plane determines the quality of the extrapolation for $F_{2N}(x)$ in the physical x plane. For $F(x;\alpha)$ in (3), the *exact* Borel transform is

$$B(p;\alpha) = \sum_{n=0}^{\infty} \frac{(-1)^n \Gamma(n-\alpha)}{\Gamma(-\alpha) n!} p^n = (1+p)^\alpha \tag{5}$$

with a branch cut on the negative p axis: $p \in (-\infty, -1]$. The closed-form expression for the diagonal Padé approximation of $B_{2N}(p)$ is:

$$\mathrm{PB}_{[N,N]}(p;\alpha) = \frac{P_N^{(\alpha,-\alpha)}\left(1+\frac{2}{p}\right)}{P_N^{(-\alpha,\alpha)}\left(1+\frac{2}{p}\right)} \tag{6}$$

$P_N^{(\alpha,\beta)}$ is the Nth Jacobi polynomial. This Padé-Borel approximation is a ratio of *polynomials*, with only pole singularities. Padé attempts to represent a cut with an interlacing set of zeros and poles [45,50,51]. We see this clearly here because Jacobi polynomial zeros lie on the real axis in the interval $(-1, 1)$, so the zeros of the denominator in (6) lie along the Borel plane cut, $p \in (-\infty, -1)$, accumulating to $p = -1$.

Away from the cut, the Padé-Borel transform $\mathrm{PB}_{[N,N]}(p;\alpha)$ in (6) is remarkably accurate. Large N asymptotics of the Jacobi polynomials quantifies this statement:

$$\frac{\mathrm{PB}_{[N,N]}(p;\alpha)}{(1+p)^\alpha} \sim \frac{I_\alpha\left(\left(N+\frac{1}{2}\right)\ln\left[\frac{\sqrt{1+p}+1}{\sqrt{1+p}-1}\right]\right)}{I_{-\alpha}\left(\left(N+\frac{1}{2}\right)\ln\left[\frac{\sqrt{1+p}+1}{\sqrt{1+p}-1}\right]\right)} \tag{7}$$

I_α is the modified Bessel function. For Borel extrapolation, small x behavior is controlled by large p behavior of the Borel transform. Eq. (7) implies $\mathrm{PB}_{[N,N]}(p;\alpha) \sim p^\alpha \left(\frac{N^2}{p}\right)^\alpha$ as $p \to +\infty$. Thus Padé-Borel is good up to $p \sim N^2$, translating to an x space extrapolation extending down to $x_{\min} \sim 1/N^2$. See Fig. 1. This explains why Padé in the Borel plane is generally more precise than Padé in the physical plane, an old empirical observation in [52].

[1] Other interesting numerical methods include summation to the least term, greatly improved by hyperasymptotics and hyperterminants [46,47], which iterate the asymptotics of the asymptotics, but these typically have a terminal non-zero error, and a direct comparison is beyond the scope of this paper.

The most interesting thing about our uniform Padé-Borel approximation (7) is the appearance of the conformally mapped variable z:

$$z = \frac{\sqrt{1+p}-1}{\sqrt{1+p}+1} \quad \longleftrightarrow \quad p = \frac{4z}{(1-z)^2} \tag{8}$$

which maps the cut Borel p plane to the interior of the unit disc, $|z| < 1$. Conformal maps are well-known tools for physical resummation problems [5–17], but the result (7) now explains why and how it works so well: *the conformal variable is the natural variable of large order Padé asymptotics*. This is a general property of Padé approximations [45,50,51], not just for the function $F(x;\alpha)$ in (3).

Another common physical extrapolation, Taylor-Conformal-Borel, does not use Padé, but conformally maps the truncated Borel function to the unit disc in z, re-expands and maps back to the Borel p plane [6,8,13]. See Fig. 6 for an illustrative comparison. This similarity arises from comparing the asymptotics of the Padé-Borel expression in (6) with the Padé of the Taylor-Conformal expansion in (A.9) [45]. Our methods show that this procedure is comparable to Padé-Borel, with $x_{\rm min}$ also scaling as $1/N^2$, but subleading terms tend to make it slightly better.

A significantly better Borel extrapolation [5,12,53–55] combines the conformal map with a Padé approximation in the conformal z variable, before mapping back to the Borel p plane. We show that this simple extra Padé step yields a further factor of $1/N^2$ improvement in the extrapolation down towards $x = 0$. The closed-form diagonal Padé approximant is now:

$$\mathrm{PCB}_{[N,N]}(p;\alpha) = \frac{P_N^{(2\alpha,-2\alpha)}\left(\frac{\sqrt{1+p}+1}{\sqrt{1+p}-1}\right)}{P_N^{(-2\alpha,2\alpha)}\left(\frac{\sqrt{1+p}+1}{\sqrt{1+p}-1}\right)} \tag{9}$$

$P_N^{(\alpha,\beta)}$ is again the Nth Jacobi polynomial. Uniform large N asymptotics yields (see App. A):

$$\frac{\mathrm{PCB}_{[N,N]}(p;\alpha)}{(1+p)^{\alpha}} \sim \frac{I_{2\alpha}\left(\left(N+\frac{1}{2}\right)\ln[h(p)]\right)}{I_{-2\alpha}\left(\left(N+\frac{1}{2}\right)\ln[h(p)]\right)} \tag{10}$$

where the argument now involves the function $h(p) = \left(\frac{\sqrt{1+p}+1}{\sqrt{1+p}-1}\right)\frac{((1+p)^{1/4}+1)^2}{(\sqrt{1+p}+1)}$, and the Bessel index is 2α. Contrast (10) with the Padé-Borel result (7). The small x behavior is controlled by the large p behavior of the Borel transform. As $p \to +\infty$, we find $\mathrm{PCB}_{[N,N]}(p;\alpha) \sim p^{\alpha}\left(\frac{N^4}{p}\right)^{\alpha}$. Thus $\mathrm{PCB}_{[N,N]}(p;\alpha)$ extends out to large p scaling like N^4, corresponding to extrapolation in x down to $x_{\rm min}$ scaling as $1/N^4$. See Fig. 1. This represents a dramatic improvement in the range of extrapolation, using exactly the same input coefficients, even when this number of input coefficients is only of the order of 10.

Since the large N asymptotics (7), (10) are uniform in p, we can probe the quality of the extrapolations throughout the complex x plane. The most dramatic superiority of the Padé-Conformal-Borel extrapolation is seen in the non-perturbative region near the negative x axis, which is "as far as possible" from the starting perturbative expansion region $x \to +\infty$, on the positive x axis. This region is governed by the Borel transform near the Borel plane cut: $p \in (-\infty, -1]$. Both Padé-Borel and Taylor-Conformal-Borel have unphysical oscillations near the cut, while the Padé-Conformal-Borel transform is extremely accurate. See Fig. 2. This is because the argument of the Jacobi polynomials in (9) is $\frac{1}{z}$, the *inverse* of the conformal variable z in (8). The Jacobi zeros lie in the interval $(-1, 1)$, so z lies *outside* the conformal unit disc. Therefore the Padé singularities are on the next Riemann sheet when mapped back to the Borel plane. In other words, the Padé-Conformal-Borel transform has no poles or singularities along the cut. See Fig. 2.

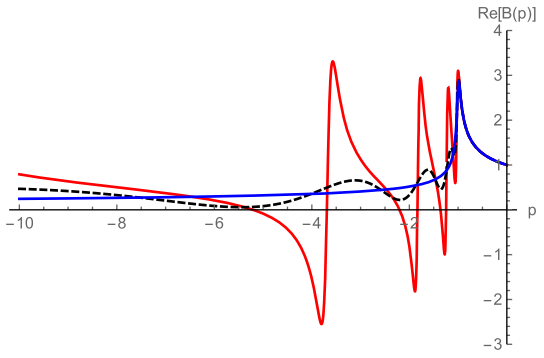

Fig. 2. Real part of the $N = 5$ Borel transform at a grazing angle $.01\pi$ above the Borel cut. The Padé-Conformal-Borel transform matches the exact Borel function [blue curve]. The Padé-Borel (red) and Taylor-Conformal-Borel (black-dashed) approximations show unphysical oscillations near the cut.

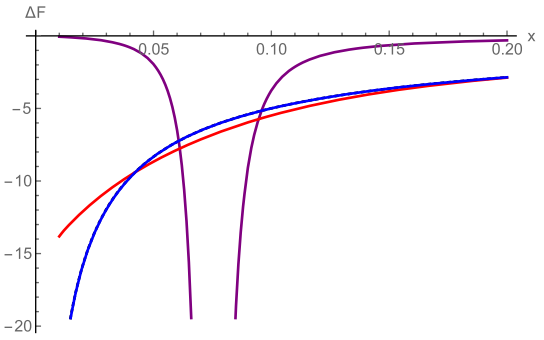

Fig. 3. The purple, red and blue curves show the non-perturbative Stokes jump (4), for x-Padé, Padé-Borel and Padé-Conformal-Borel extrapolations ($N = 5$), resp. Padé-Conformal-Borel agrees with the exact Stokes jump in (4). Padé in x and Padé-Borel fail at small $|x|$ due to unphysical poles.

It is therefore far better representing non-perturbative Stokes phenomena: see Fig. 3. With just 10 perturbative input coefficients, generated from an asymptotic expansion about $x \to +\infty$, the Padé-Conformal-Borel extrapolation encodes the exact Stokes jump (4), even at very small $|x|$. The Padé-Borel extrapolation fails at small $|x|$, due to unphysical poles on the Borel cut. The x space Padé extrapolation is much worse, due to unphysical poles on the x space cut.

Our quantitative extrapolation analysis for the physically motivated model function $F(x;\alpha)$ in (3) generalizes to all resurgent functions, which are universal in physical applications [45]. This is because resurgent functions have isolated algebraic or logarithmic Borel branch points, and physical resurgent functions tend to have relatively simple Borel plane structure. But even for simple structures with multiple singularities, Padé-Borel fails because it puts unphysical poles on artificial arcs along or crossing the Borel integration axis [45,50,51], while Padé-Conformal-Borel does not. See Figs. 2, 4, 5. A further advantage is that, generically for nonlinear problems, each Borel singularity p_k is repeated at integer multiples along the direction $\arg(p_k)$: a physical "multi-instanton" expansion or renormalon structure. Here Padé-Borel fails because it places unphysical poles along this direction (Figs. 4, 5), thereby obscuring the further resurgent Borel singularities. In contrast, Padé-Conformal-Borel can accurately represent such a situation of aligned branch points (overlapping branch cuts), resolving higher resurgent singularities. This has been demonstrated to high precision for the Painlevé I equation [55], which describes the double-scaling limit of matrix models for 2d quantum gravity [56].

We illustrate these points with two physical examples from quantum mechanics and quantum field theory. (Two further quantum field theoretic applications are in [57,58]). In each case, there

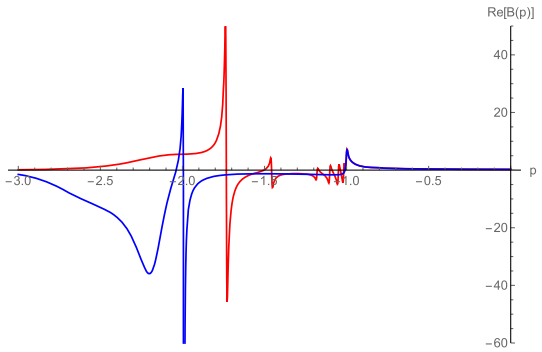

Fig. 4. The real part of the Borel transform of the ground state energy for the quartic anharmonic oscillator, on the negative Borel axis along which there are physical singularities at integer multiples of the leading one at $p = -1$. The Padé-Borel transform (red curve) introduces spurious singularities beyond the leading one, and is unable to resolve the second. The Padé-Conformal-Borel transform (blue curve) smoothly resolves the first two singularities.

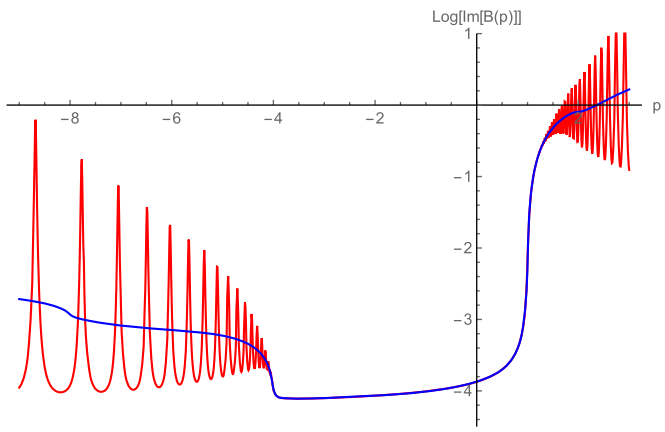

Fig. 5. The logarithm of the imaginary part of the Borel transform of the divergent perturbative strong coupling expansion of the cusp anomalous dimension. There are physical singularities along the Borel axis at integer multiples of the leading negative one at $p = -4$ and leading positive one at $p = +1$. The Padé-Conformal-Borel transform (blue) smoothly resolves the first two singularities, on both the negative and positive Borel axis. The Padé-Borel transform (red) introduces spurious singularities beyond the leading one, and is unable to resolve the second, in both directions.

is an infinite set of Borel singularities, but we can apply our analysis in the vicinity of each. The quartic anharmonic oscillator is an important physical paradigm of the study of asymptotic series and Padé methods [42,44,52]. Indeed, [52] contains an early explicit instance of the Padé-Borel method. In Fig. 4 we consider the perturbative expansion of the ground state energy for the Hamiltonian $H = \frac{p^2}{2} + \frac{1}{2}x^2 + \lambda x^4$, and plot the associated Borel transform (the real part thereof) just above the negative Borel p axis, along which there are physical singularities at all integer multiples of the leading singularity, normalized to be at $p = -1$. These are the singularities on the first Riemann sheet corresponding to the physical instability when $\lambda \to -\lambda$. We take 40 input coefficients, generated from the BenderWu package [59]. Fig. 4 shows that the Padé-Borel method (red curve) resolves the leading Borel singularity, but beyond $p = -1$ Padé-Borel places artificial poles in an attempt to represent the leading cut, and so is unable to resolve the second resurgent singularity at $p = -2$. By contrast, the Padé-Conformal-Borel method (blue curve), with exactly the same input coefficients, has no such spurious poles between $p = -1$ and $p = -2$, and furthermore is able to resolve the second Borel singularity. Taking more coefficients allows one to resolve further Borel singularities. This added precision leads to improved resummations of the ground state energy, and also to accurate extractions of non-perturbative information due to the precision near the cuts.

A physical example from quantum field theory is the cusp anomalous dimension, denoted $\Gamma(g)$, in maximally supersymmetric Yang-Mills theory in 4 spacetime dimensions. This quantity satisfies a system of non-linear integral equations, the Beisert-Eden-Staudacher (BES) equations [60]. It is convergent at weak coupling, but divergent at strong coupling [61]. Its resurgent properties have been studied in [62,63]: $\Gamma(g)$ has a trans-series structure, as a sum over an infinite tower of saddles, and the fluctuation about each saddle is an asymptotic series. Padé-Borel analysis of the fluctuations about the first and second saddles, suggests an asymmetric Borel plane structure, with leading singularities at $p = +1$ and $p = -4$, while for the fluctuations about the third saddle the leading singularities are at $p = \pm 1$ [62,63]. Fig. 5 shows the logarithm of the imaginary part of the Borel transform of the divergent perturbative strong coupling expansion of the cusp anomalous dimension, based on 180 input coefficients (from [63]) [the fluctuation about the perturbative saddle], plotted along the Borel axis along which there are physical singularities at integer multiples of the leading negative one at $p = -4$ and the leading positive one at $p = +1$. We plot the logarithm in order to be able to show the positive and negative singularities on the same scale. We see that each of the Padé-Borel and Padé-Conformal-Borel transforms resolves the leading singularity on both the positive and negative Borel axis, but that the Padé-Borel method fails beyond these leading singularities because it places spurious poles in an attempt to represent the leading singularities. By contrast, the Padé-Conformal-Borel method produces no such unphysical singularities along the cut, and furthermore resolves the second singularity on both the positive and negative Borel axis. In fact, higher singularities can also be resolved with this same input data.

To summarize, we have given new sharp estimates of the precision obtained by a variety of extrapolation methods, in the vicinity of an isolated branch cut Borel singularity. Dramatic, and quantifiable, improvements can be made based on exactly the same input data. In [45] we will prove analogous results for any resurgent function f: the optimal reconstruction accuracy is obtained from the truncated Taylor series of $f \circ \psi^{-1}$, where ψ is a uniformization map from the Riemann surface of f onto the unit disk, with $\psi(0) = 0$. The resurgence perspective also leads to new approximation procedures [45]. *Singularity elimination* allows one to probe the vicinity of any given Borel singularity with extreme sensitivity. This can be applied not just in the Borel plane, but also to analyze branch cut singularities in the physical plane, e.g. in the study of phase transitions and critical exponents [2–4,9,10]. The *capacity theory* interpretation of Padé in terms of a minimal capacitor [50,51], by which poles are placed as charges on a graph of *minimal capacitance*, leads to new physically motivated methods to move poles out of the way, to break unphysical pole arcs, and to zoom in on a chosen singularity, leading to dramatic increases in precision. We anticipate that recent numerical conformal mapping algorithms [64] will be useful for analysis of realistic physical models. Further physical applications will be described elsewhere.

Declaration of competing interest

The authors declare that they have no known competing financial interests or personal relationships that could have appeared to influence the work reported in this paper.

Acknowledgements

This work is supported by The U.S. Department of Energy, Office of High Energy Physics, Award DE-SC0010339. We thank D. Dorigoni for sharing expansion coefficients for the cusp anomalous dimension.

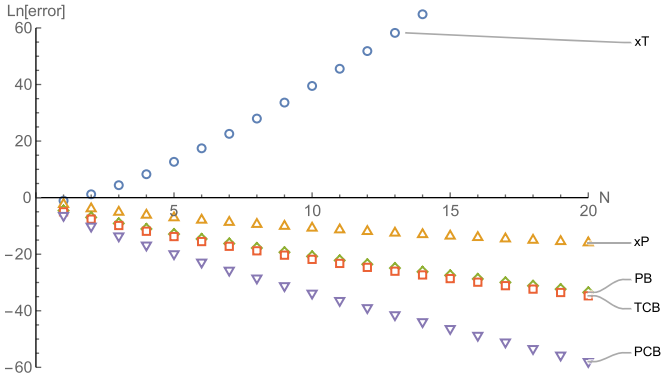

Fig. 6. Logarithm of the fractional error in the extrapolation of $F(x=1;-\frac{1}{3})$, as a function of the input truncation order parameter N, extrapolated from a perturbative expansion at $x=+\infty$ down to a fixed reference value $x=1$. The plots show the truncated series (xT), x-space Padé (xP), Padé-Borel (PB), Taylor-Conformal-Borel (TCB) and Padé-Conformal-Borel (PCB) extrapolations, respectively. These curves match well with the analytic large N results in Eqs. (A.5), (A.8) and (A.12).

Appendix A. Details of asymptotic results

This Appendix presents further technical details of the analytic comparisons between the five different extrapolation methods studied in this paper. Table 1 summarizes at a glance how the minimal x at which a chosen level of precision can be achieved scales with the truncation order parameter N. Fig. 6 displays the logarithm of the fractional error, as a function of the truncation order parameter N, in the extrapolation from $x=+\infty$ down to a fixed reference value, chosen here to be $x=1$. The truncated series at fixed x gets dramatically worse for larger N, while all other extrapolations improve in precision with increasing N.

1. Truncated series: For a truncated asymptotic series with coefficients growing like $n!$, the optimal truncation order is at $N\sim x$ [48], so if N is fixed we can achieve a reasonable precision only for x extrapolated from $x=+\infty$ down to some $x_{\rm min}$ that scales with N as $x_{\rm min}\sim N$.

2. x-Padé: An improved extrapolation is achieved by computing a Padé approximant of the truncated asymptotic series in the physical $1/x$ variable. For our physical test function $F(x;\alpha)=x^{-1-\alpha}\,e^x\Gamma(1+\alpha,x)$, which has Bender-Wu-Lipatov asymptotics [42–44], this Padé approximant can be computed in closed form, which leads to precise asymptotic precision estimates. We find the closed-form:

$$P_{[N-1,N]}(F(x;\alpha))=\frac{R_{N-1}(x;\alpha)}{S_N(x;\alpha)} \tag{A.1}$$

where the polynomials $R_{N-1}(x;\alpha)$ and $S_N(x;\alpha)$ are in terms of Laguerre polynomials:

$$S_N(x;\alpha)=N!\,L_N^{(-1-\alpha)}(-x) \tag{A.2}$$

$$R_{N-1}(x;\alpha)= \sum_{j=0}^{\left[\frac{N-1}{2}\right]}\frac{\Gamma(N-j)\Gamma(1+\alpha)}{\Gamma(1+\alpha-j)}\,L_{N-1-2j}^{(2j+1-\alpha)}(-x) \tag{A.3}$$

A general feature of Padé is that the difference between successive near-diagonal approximants can be expressed in terms of successive denominator factors [48,49]. Here this reads:

$$P_{[N,N+1]}(F(x;\alpha))-P_{[N-1,N]}(F(x;\alpha)) = \frac{\Gamma(N-\alpha)}{\Gamma(-\alpha)\,(N+1)!\,L_{N+1}^{(-1-\alpha)}(-x)\,L_N^{(-1-\alpha)}(-x)} \tag{A.4}$$

The large N asymptotics of Laguerre polynomials therefore leads to a sharp estimate for the fractional error:

$$\frac{F(x;\alpha)-P_{[N-1,N]}(F(x;\alpha))}{F(x;\alpha)}\sim e^{-\sqrt{8\,N\,x}} \tag{A.5}$$

Thus, for a chosen level of precision, one can extrapolate from $x=+\infty$ down to $x_{\rm min}$ which scales with the truncation order as $x_{\rm min}\sim\frac{1}{N}$. This is a significant improvement over the naive truncated series. See Fig. 6. Recall that exactly the same input data is used.

3. Padé-Borel: Instead of a Padé approximation in the x plane, we can use a Padé approximation in the Borel p plane: we thereby analytically continue the truncated Borel transform function, $B_{2N}(p)=\sum_{n=0}^{2N}\frac{a_n}{n!}p^n$, instead of the truncated series (1). Padé is a nonlinear operation, so it does not commute with the Borel transform step. It had been observed empirically in the analysis of the spectrum of the quantum anharmonic oscillator [52], that a Padé approximation in the Borel plane produced more precise results than a Padé approximation in the coupling plane. See also [65]. Here we explain why this is the case, and furthermore we quantify the degree of improvement.

For the physical model function $F(x;\alpha)$ in (3), the closed-form Padé-Borel transform is expressed as a ratio of Jacobi polynomials in (6), and the uniform large N limit is presented in Eq. (7) as a ratio of modified Bessel functions. This large N limit is remarkably precise even for small values of N. At small p, which governs the large x behavior of the extrapolated function in the physical x plane, we find a fractional error:

$$\begin{aligned}&\frac{(1+p)^\alpha-{\rm PB}_{[N,N]}(p;\alpha)}{(1+p)^\alpha}\\ &\sim 2\sin(\pi\alpha)\left(\frac{\sqrt{1+p}-1}{\sqrt{1+p}+1}\right)^{2N+1}\\ &\sim 2\sin(\pi\alpha)\left(\frac{p}{4}\right)^{2N+1}\end{aligned} \tag{A.6}$$

Note the appearance of the conformal variable z from (8) in this limit. This is general [45,50,51]. In the opposite limit, as $p\to+\infty$, which governs the small x behavior of the extrapolated function in the physical x plane, we have:

$$\begin{aligned}{\rm PB}_{[N,N]}(p;\alpha)&\sim\frac{\Gamma(1-\alpha)}{\Gamma(1+\alpha)}\frac{\Gamma(N+1+\alpha)}{\Gamma(N+1-\alpha)}\\ &\quad\times\left(1+\frac{2\alpha N(N+1)}{(\alpha^2-1)}\frac{1}{p}+\dots\right)\\ &\sim\frac{\Gamma(1-\alpha)}{\Gamma(1+\alpha)}\,p^\alpha\left(\frac{N^2}{p}\right)^\alpha\end{aligned} \tag{A.7}$$

In other words, while the true Borel transform has large p behavior $B(p;\alpha)\sim p^\alpha$, the Padé-Borel approximation behaves as ${\rm PB}(p;\alpha)\sim N^{2\alpha}$, implying that in a uniform large N and large p limit, the Borel variable p scales with N^2. Thus, there is good agreement between ${\rm PB}(p;\alpha)$ and the true Borel transform up to a p value that scales as N^2 with the truncation order. A large N analysis of the Laplace integral, $F_{2N}(x)=\int_0^\infty dp\,e^{-px}B_{2N}(p)$, using the uniform asymptotics in (7) leads to the fractional error of the Padé-Borel extrapolation in the physical x plane:

$$\begin{aligned}&{\rm fractional\ error}_{\rm PB}(x,N;\alpha)\\ &\sim 2\sqrt{\frac{\pi}{3}}\frac{\sin(\pi\alpha)}{\sqrt{x}}\left(\frac{2N}{x}\right)^{(2\alpha+1)/3}\\ &\quad\times\exp\left[-3\left(4N^2x\right)^{1/3}+\frac{x}{3}+\dots\right]\end{aligned} \tag{A.8}$$

This confirms that the leading behavior has $x_{\min}$ scaling with $\frac{1}{N^2}$, and specifies the subleading corrections, which agree well with the numerical results in Fig. 1. Note that the dependence on the cut exponent α is subleading.

4. Taylor-Conformal-Borel: Another approximation method, of precision comparable with the Padé-Borel method, does not use a Padé approximation, but instead makes a conformal map in the Borel plane [6,8,13]. This Taylor-Conformal-Borel extrapolation consists of re-expanding the Borel transform function in the conformal variable to the same order as the original truncated series. This can then be mapped back to the original Borel plane to perform the integral, or equivalently the integral can be done inside the unit disc of the conformal z plane. For our model function $F(x;\alpha)$ in (3), the mapped Taylor-Conformal-Borel transform has the explicit closed-form expression

$$\mathrm{TCB}_{2N}(p;\alpha) = \sum_{l=0}^{2N} \binom{2\alpha}{l} \times {}_2F_1(-l, 2\alpha, 1-l+2\alpha; -1) \left(\frac{\sqrt{1+p}-1}{\sqrt{1+p}+1}\right)^l \tag{A.9}$$

enabling rigorous estimates of the precision [45]. The resulting precision is comparable with, but due to sub-leading terms is generally slightly better than, the Padé-Borel extrapolation described above. See Fig. 6 and Table 1.

5. Padé-Conformal-Borel: A far better extrapolation, which combines the advantages of the Padé-Borel method with those of conformal mapping, is obtained by adding a simple extra step of Padé approximation in the conformally mapped z plane before mapping back to the Borel plane [5,12,53–55]. This straightforward extra Padé step leads to a dramatic further improvement in the resulting extrapolation. See Figs. 1 and 6, and Table 1.

For the physical model function $F(x;\alpha)$ in (3), the closed-form Padé-Conformal-Borel transform is expressed as a ratio of Jacobi polynomials in (9), and the uniform large N limit is presented in Eq. (10) as a ratio of modified Bessel functions. This large N limit is remarkably precise even for small values of N. At small p, which governs the large x behavior of the extrapolated function in the physical x plane, we have a fractional error:

$$\begin{aligned} &\frac{(1+p)^\alpha - \mathrm{PCB}_{[N,N]}(p;\alpha)}{(1+p)^\alpha} \\ &\sim 2\sin(2\pi\alpha)\left(\frac{\sqrt{1+p}-1}{(1+(1+p)^{1/4})^2}\right)^{2N+1} \\ &\sim 2\sin(2\pi\alpha)\left(\frac{p}{8}\right)^{2N+1} \quad , \quad p \to 0 \end{aligned} \tag{A.10}$$

There are two important differences compared to the corresponding result for the Padé-Borel transform in (A.6). First, the branch cut exponent α appears as $\sin(2\pi\alpha)$ instead of $\sin(\pi\alpha)$, reflecting the fact that for a square root branch cut the conformally mapped function is already rational, so the Padé step is in fact exact. The other difference is the different function of p in (A.10). This leads to a further gain of a factor of $1/4^N$ in the precision at small p, and hence a similar gain in precision at large x.

In the opposite limit, as $p \to +\infty$, which governs the small x behavior of the extrapolated function in the physical x plane, we find:

$$\begin{aligned} \mathrm{PCB}_{[N,N]}(p;\alpha) &\sim \frac{\Gamma(1-2\alpha)}{\Gamma(1+2\alpha)} \frac{\Gamma(N+1+2\alpha)}{\Gamma(N+1-2\alpha)} \\ &\times \left(1 + \frac{4\alpha N(N+1)}{(4\alpha^2-1)} \frac{1}{\sqrt{p}} + \dots\right) \\ &\sim \frac{\Gamma(1-2\alpha)}{\Gamma(1+2\alpha)} p^\alpha \left(\frac{N^4}{p}\right)^\alpha \end{aligned} \tag{A.11}$$

Thus $\mathrm{PCB}_{[N,N]}(p;\alpha)$ extends accurately out to large p scaling like N^4, which translates to a high quality extrapolation in x down to $x_{\min}$ scaling like $1/N^4$. See Figs. 1 and 6, and Table 1. A large N analysis of the Borel integral back to the physical x plane, using the uniform asymptotics in (10), leads to the fractional error of the Padé-Conformal-Borel extrapolation in the physical x plane:

$$\begin{aligned} &\text{fractional error}_{\mathrm{PCB}}(x, N; \alpha) \sim \\ &2\sqrt{\frac{2\pi}{5}} \frac{\sin(2\pi\alpha)}{\sqrt{x}} \left(\frac{N}{x}\right)^{2(2\alpha+1)/5} \\ &\times \exp\left[-5\left(N^4 x\right)^{\frac{1}{5}} - \frac{4}{3N^2}(N^4 x)^{\frac{3}{5}} + \frac{3x}{5} + \dots\right] \end{aligned} \tag{A.12}$$

This confirms that the leading behavior has $x_{\min}$ scaling with $\frac{1}{N^4}$, and specifies the subleading corrections, which agree well with the numerical results shown in Fig. 1.

References

[1] W.R. Frazer, Applications of conformal mapping to the phenomenological representation of scattering amplitudes, Phys. Rev. 123 (1961) 2180.
[2] D.L. Hunter, G.A. Baker Jr., Methods of series analysis. I. Comparison of current methods used in the Theory of Critical Phenomena, Phys. Rev. B 7 (1973) 3346.
[3] M.E. Fisher, Critical point phenomena – the role of series expansions, Rocky Mt. J. Math. 4 (1974) 181–201.
[4] D.S. Gaunt, A.J. Guttmann, Asymptotic analysis of coefficients, in: C. Domb, M.S. Green (Eds.), Phase Transitions and Critical Phenomena, Vol. 3, Academic Press, 1974.
[5] J.C. Le Guillou, J. Zinn-Justin, Critical exponents from field theory, Phys. Rev. B 21 (1980) 3976.
[6] D.I. Kazakov, D.V. Shirkov, O.V. Tarasov, Analytical continuation of perturbative results of the $g\phi^4$ model into the region g is greater than or equal to 1, Theor. Math. Phys. 38 (1979) 9.
[7] R. Guida, J. Zinn-Justin, Critical exponents of the N vector model, J. Phys. A 31 (1998) 8103, arXiv:cond-mat/9803240.
[8] J. Fischer, On the role of power expansions in quantum field theory, Int. J. Mod. Phys. A 12 (1997) 3625, arXiv:hep-ph/9704351.
[9] J. Zinn-Justin, Quantum field theory and critical phenomena, Int. Ser. Monogr. Phys. 113 (2002) 1.
[10] H. Kleinert, Critical Properties of Phi 4 Theories, World Scientific, Singapore, 2004.
[11] M.A. Stephanov, QCD critical point and complex chemical potential singularities, Phys. Rev. D 73 (2006) 094508, arXiv:hep-lat/0603014.
[12] E. Caliceti, M. Meyer-Hermann, P. Ribeca, A. Surzhykov, U.D. Jentschura, From useful algorithms for slowly convergent series to physical predictions based on divergent perturbative expansions, Phys. Rep. 446 (2007) 1, arXiv:0707.1596.
[13] M. Serone, G. Spada, G. Villadoro, $\lambda\phi^4$ Theory I: the symmetric phase beyond NNNNNNNNLO, J. High Energy Phys. 1808 (2018) 148, arXiv:1805.05882;
M. Serone, G. Spada, G. Villadoro, $\lambda\phi_2^4$ theory II. The broken phase beyond NNNN(NNNN)LO, J. High Energy Phys. (1905) 047, arXiv:1901.05023, 2019.
[14] R. Rossi, T. Ohgoe, K. Van Houcke, F. Werner, Resummation of diagrammatic series with zero convergence radius for strongly correlated fermions, Phys. Rev. Lett. 121 (13) (2018) 130405, arXiv:1802.07717.
[15] K. Van Houcke, F. Werner, R. Rossi, High-precision numerical solution of the Fermi polaron problem and large-order behavior of its diagrammatic series, Phys. Rev. B 101 (2014) 045134, arXiv:1402.4015.
[16] R.E.V. Profumo, C. Groth, L. Messio, O. Parcollet, X. Waintal, Quantum Monte Carlo for correlated out-of-equilibrium nanoelectronic devices, Phys. Rev. B 91 (2015) 245154, arXiv:1504.02132.
[17] C. Bertrand, S. Florens, O. Parcollet, X. Waintal, Reconstructing nonequilibrium regimes of quantum many-body systems from the analytical structure of perturbative expansions, Phys. Rev. X 9 (2019) 041008, arXiv:1903.11646.
[18] V. Skokov, K. Morita, B. Friman, Mapping the phase diagram of strongly interacting matter, Phys. Rev. D 83 (2011) 071502.
[19] N. Clisby, B.M. McCoy, Ninth and tenth order virial coefficients for hard spheres in D dimensions, J. Stat. Phys. 122 (2006) 15–57.
[20] J. Ecalle, Les fonctions resurgentes; Vols. 1-3, Pub. Math. d'Orsay, 1981–1985.
[21] E. Delabaere, F. Pham, Resurgent methods in semiclassical asymptotics, Ann. Inst. Henri Poincaré 71 (1999) 1–94.
[22] O. Costin, Asymptotics and Borel Summability, Chapman and Hall/CRC, 2008.

[23] J. Zinn-Justin, U.D. Jentschura, Multi-instantons and exact results I: conjectures, WKB expansions, and instanton interactions, Ann. Phys. 313 (2004) 197, arXiv:quant-ph/0501136;
J. Zinn-Justin, U.D. Jentschura, Multi-instantons and exact results II: specific cases, higher-order effects, and numerical calculations, Ann. Phys. 313 (2004) 269, arXiv:quant-ph/0501137.
[24] M. Mariño, Nonperturbative effects and nonperturbative definitions in matrix models and topological strings, J. High Energy Phys. 0812 (2008) 114, arXiv:0805.3033.
[25] S. Garoufalidis, A. Its, A. Kapaev, M. Marino, Asymptotics of the instantons of Painlevé I, Int. Math. Res. Not. 2012 (3) (2012) 561, arXiv:1002.3634.
[26] I. Aniceto, R. Schiappa, M. Vonk, The resurgence of instantons in string theory, Commun. Number Theory Phys. 6 (2012) 339, arXiv:1106.5922.
[27] G.V. Dunne, M. Ünsal, Resurgence and trans-series in quantum field theory: the CP(N-1) model, J. High Energy Phys. 1211 (2012) 170, arXiv:1210.2423.
[28] M. Mariño, Instantons and Large N, Cambridge University Press, 2015.
[29] A. Grassi, M. Marino, S. Zakany, Resumming the string perturbation series, J. High Energy Phys. 1505 (2015) 038, arXiv:1405.4214.
[30] G. Başar, G.V. Dunne, Resurgence and the Nekrasov-Shatashvili limit: connecting weak and strong coupling in the Mathieu and Lamé systems, J. High Energy Phys. 1502 (2015) 160, arXiv:1501.05671.
[31] T. Misumi, M. Nitta, N. Sakai, Resurgence in sine-Gordon quantum mechanics: exact agreement between multi-instantons and uniform WKB, J. High Energy Phys. 1509 (2015) 157, arXiv:1507.00408.
[32] G.V. Dunne, M. Ünsal, New nonperturbative methods in quantum field theory: from large-N orbifold equivalence to bions and resurgence, Annu. Rev. Nucl. Part. Sci. 66 (2016) 245, arXiv:1601.03414.
[33] S. Gukov, M. Marino, P. Putrov, Resurgence in complex Chern-Simons theory, arXiv:1605.07615.
[34] A. Ahmed, G.V. Dunne, Transmutation of a trans-series: the Gross-Witten-Wadia phase transition, J. High Energy Phys. 1711 (2017) 054, arXiv:1710.01812.
[35] I. Aniceto, G. Basar, R. Schiappa, A primer on resurgent transseries and their asymptotics, Phys. Rep. 809 (2019) 1, arXiv:1802.10441.
[36] A. Grassi, J. Gu, Argyres-Douglas theories, Painlevé II and quantum mechanics, J. High Energy Phys. 1902 (2019) 060, arXiv:1803.02320.
[37] M.C.N. Cheng, S. Chun, F. Ferrari, S. Gukov, S.M. Harrison, 3d Modularity, J. High Energy Phys. 1910 (2019) 010, arXiv:1809.10148.
[38] J.E. Andersen, W.E. Petersen, Resurgence analysis of quantum invariants: Seifert manifolds and surgeries on the figure eight knot, arXiv:1811.05376.
[39] K. Ito, M. Mariño, H. Shu, TBA equations and resurgent quantum mechanics, J. High Energy Phys. 1901 (2019) 228, arXiv:1811.04812.
[40] M. Mariño, T. Reis, Resurgence for superconductors, J. Stat. Mech. (2019) 123102, arXiv:1905.09569.
[41] F.J. Dyson, Divergence of perturbation theory in quantum electrodynamics, Phys. Rev. 85 (1952) 631.
[42] C.M. Bender, T.T. Wu, Anharmonic oscillator, Phys. Rev. 184 (1969) 1231;
C.M. Bender, T.T. Wu, Anharmonic oscillator. 2: a study of perturbation theory in large order, Phys. Rev. D 7 (1973) 1620.
[43] L.N. Lipatov, Divergence of the perturbation theory series and the quasiclassical theory, Sov. Phys. JETP 45 (1977) 216.
[44] J.C. Le Guillou, J. Zinn-Justin, Large Order Behavior of Perturbation Theory, North-Holland, Amsterdam, 1990.
[45] O. Costin, G.V. Dunne, to appear.
[46] M.V. Berry, C.J. Howls, Hyperasymptotics, Proc. R. Soc. A 430 (1990) 653–668;
M.V. Berry, C.J. Howls, Hyperasymptotics for integrals with saddles, Proc. R. Soc. A 434 (1991) 657–675.
[47] A.B. Olde Daalhuis, Hyperterminants I, J. Comput. Appl. Math. 76 (1996) 255–264;
A.B. Olde Daalhuis, Hyperterminants II, J. Comput. Appl. Math. 89 (1998) 87–95;
A.B. Olde Daalhuis, Hyperasymptotics and hyperterminants: exceptional cases, J. Comput. Appl. Math. 233 (2009) 555–563.
[48] C.M. Bender, S.A. Orszag, Advanced Mathematical Methods for Scientists and Engineers, McGraw Hill, New York, 1978.
[49] G.A. Baker, P. Graves-Morris, Padé Approximants, Cambridge University Press, 2009.
[50] G. Szegö, Orthogonal Polynomials, American Mathematical Society, 1939;
U. Grenander, G. Szegö, Toeplitz Forms and Their Applications, Univ. California Press, Berkeley, 1958.
[51] H.R. Stahl, Sets of minimal capacity and extremal domains, arXiv:1205.3811.
[52] S. Graffi, V. Grecchi, B. Simon, Borel summability: application to the anharmonic oscillator, Phys. Lett. B 32 (1970) 631–634.
[53] A.H. Mueller, The QCD perturbation series, in: P.M. Zerwas, H.A. Kastrup (Eds.), QCD 20 Years Later, World Scientific, NJ, 1993.
[54] I. Caprini, J. Fischer, G. Abbas, B. Ananthanarayan, Perturbative expansions in QCD improved by conformal mappings of the Borel plane, in: Perturbation Theory: Advances in Research and Applications, Nova Science Publishers, 2018, arXiv:1711.04445.
[55] O. Costin, G.V. Dunne, Resurgent extrapolation: rebuilding a function from asymptotic data. Painlevé I, J. Phys. A 52 (44) (2019) 445205, arXiv:1904.11593.
[56] P. Di Francesco, P.H. Ginsparg, J. Zinn-Justin, 2-D gravity and random matrices, Phys. Rep. 254 (1995) 1, arXiv:hep-th/9306153.
[57] N.A. Dondi, G.V. Dunne, M. Reichert, F. Sannino, Towards the QED beta function and renormalons at $1/N_f^2$ and $1/N_f^3$, Phys. Rev. D (2020), arXiv:2003.08397, in press.
[58] M. Borinsky, G.V. Dunne, Non-perturbative completion of Hopf-algebraic Dyson-Schwinger equations, Nucl. Phys. B 957 (2020) 115096, arXiv:2005.04265.
[59] T. Sulejmanpasic, M. Ünsal, Aspects of perturbation theory in quantum mechanics: the BenderWu Mathematica package, Comput. Phys. Commun. 228 (2018) 273–289, arXiv:1608.08256.
[60] N. Beisert, B. Eden, M. Staudacher, Transcendentality and crossing, J. Stat. Mech. 0701 (2007) P01021, arXiv:hep-th/0610251.
[61] B. Basso, G.P. Korchemsky, J. Kotanski, Cusp anomalous dimension in maximally supersymmetric Yang-Mills theory at strong coupling, Phys. Rev. Lett. 100 (2008) 091601, arXiv:0708.3933.
[62] I. Aniceto, The resurgence of the cusp anomalous dimension, J. Phys. A 49 (2016) 065403, arXiv:1506.03388.
[63] D. Dorigoni, Y. Hatsuda, Resurgence of the cusp anomalous dimension, J. High Energy Phys. 1509 (2015) 138, arXiv:1506.03763.
[64] A. Gopal, L.N. Trefethen, Representation of conformal maps by rational functions, Numer. Math. 142 (2019) 359–382, arXiv:1804.08127.
[65] J.R. Ellis, E. Gardi, M. Karliner, M.A. Samuel, Pade approximants, Borel transforms and renormalons: the Bjorken sum rule as a case study, Phys. Lett. B 366 (1996) 268, arXiv:hep-ph/9509312.